Chapter 10
Modelling the Movements of Organisms: From Cell Migration to Bumblebee Flights to Foraging Sea Turtles

Rainer Klages, Norberto Lucero-Azuara, Vijay Kumar, Alessia Gentili, Perla A. R. Torres, Christophe Eizaguirre, Giorgio Volpe, and Vladimir V. Palyulin

10.1 Introduction

Movements of organisms living at very different spatio-temporal scales, from migrating in the microworld to foraging at the surface of the Earth, exemplify the intrinsic complexity of nature. Figure 10.1 depicts three examples: White blood cells *(Neutrophil granulocytes)* crawling along a chemical gradient [1]; a bumblebee *(Bombus terrestris)* foraging in an artificial carpet of flowers in a laboratory experiment [2]; and a loggerhead sea turtle *(Caretta caretta)* swimming off the coast of West Africa [3]. All these different paths display what one may call random-looking movement patterns. Especially within the past decade, such patterns have increasingly been recorded experimentally with big data techniques for a huge variety of organisms, from bacteria [4] to insects [5], fishes, birds, mammals [6, 7] and even humans [8], to name only a few.

R. Klages (✉)
Centre for Complex Systems, School of Mathematical Sciences, Queen Mary University of London, London, UK

London Mathematical Laboratory, London, UK
e-mail: r.klages@qmul.ac.uk

N. Lucero-Azuara
Centre for Complex Systems, School of Mathematical Sciences, Queen Mary University of London, London, UK

V. Kumar · V. Palyulin
CAIT, Skolkovo Institute of Science and Technology, Bolshoy Bulwar, Moscow, Russia

A. Gentili · G. Volpe
Department of Chemistry, University College London, London, UK

P. A. R. Torres · C. Eizaguirre
School of Biological and Behavioural Sciences, Queen Mary University of London, London, UK

L. Giuggioli, P. K. Maini (eds.), *The Mathematics of Movement*,
https://doi.org/10.1007/978-3-032-00873-2_10

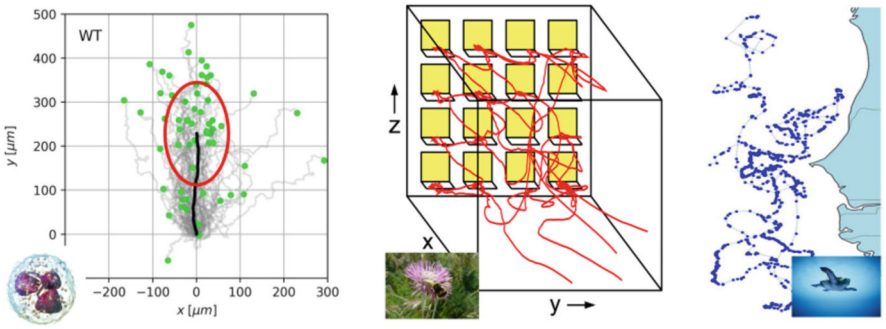

Fig. 10.1 Three examples of movement patterns across very different scales. Left: 60 neutrophil cells moving along a chemical gradient applied parallel to the y axis. The bold (black) vertical line depicts the mean position of the whole cell ensemble up to 30 min, the bold (red) ellipse the mean squared distance travelled after this time (from [1]). Centre: Part of the flight trajectory of a bumblebee foraging in an arena of artificial flowers (from [2]. Right: Path of a loggerhead sea turtle foraging in front of the coast of West Africa [9]. The insets show schematics or photos of these three organisms

Understanding these movement patterns by constructing mathematical models from data provides a fundamental challenge. The first approach for modelling the random-looking migration of organisms employed simple random walks [10, 11]. Depending on whether one was looking at the migration of organisms in the microworld or the movements of animals on macroscopic scales, this basic idea of a stochastic description of movement branched out in different directions. For example, for modelling cell migration, Langevin equations (LEs) have been used, inspired by the similarly random-looking Brownian motion of a tracer particle in a fluid [12]. Only more recently, it was found that these equations have to be generalised by including long-term memory to reproduce the persistence of cellular paths [13]. Constructing mathematical models for microswimmers like bacteria or sperm cells led yet to a different type of generalised Langevin dynamics and associated stochastic models, driven by the need to especially capture the self-propelled motion of these biological agents. The field of active particles emerged [4, 14, 15], related to the more general framework of active matter [16–18]. On the macroscale, the analysis of albatross flights led to introducing Lévy dynamics into the arsenal of stochastic methods for understanding the movements of organisms [19–21]. Lévy walks (LWs) and flights belong to an advanced class of stochastic processes exhibiting diffusive properties beyond Brownian motion, called anomalous diffusion [22–24]. In parallel, the new framework of movement ecology was formulated, which endeavours to understand organismic movement in view of important real-life biological properties like biomechanical generation of movement, perception and interaction with the environment [25–27].

The key problem which we will address in this book chapter is that, as far as biological dynamics is concerned, the theory of active particles has especially been applied to understand organismic movement on microscales. Macroscopic motion

of animals, on the other hand, has rather been modelled inspired by the stochastic theory of passively diffusing particles, either Brownian ones, as largely applied in movement ecology, or anomalously diffusing ones, as in the approach formulated by anomalous stochastic theory. In our view, the three disciplines of movement ecology, active matter and anomalous diffusion need to be suitably combined to arrive at a coherent description of movements of organisms at all scales. The framework that we develop here to achieve such a theoretical description is based on Langevin dynamics, however, generalised in a particular way which blends fundamental elements of these different three fields. We will introduce to this approach as follows: The next Sect. 10.2 briefly outlines the fields of movement ecology, active matter (viz. active particles) and anomalous diffusion by focussing on key stochastic models and their connections among each other. In Sect. 10.3, we demonstrate how to construct generalised LEs from statistical experimental data analysis of various types of biological movements. Working in a fixed Cartesian frame, we reveal features of active motion and anomalous dynamics in generalised LEs constructed for migrating cells, bumblebee flights and foraging sea turtles. Inspired by movement ecology, we then switch the perspective to a stochastic modelling in a frame comoving with a biological entity. Applied to data of bumblebee flights, this approach yields a generalised LE combining basic features of three generic active (Brownian) particle models. As we argue in Sect. 10.4, these findings suggest to use generalised Langevin dynamics in a comoving frame for modelling the movements of organisms. In the same section, we outline experimental applications of this framework and elaborate on the theoretical foundation of our generalised LE approach to formulate it on a rigorous mathematical basis. In the final Sect. 10.5, we briefly discuss the promise, main open questions and biological implications related to this approach in view of providing a general framework for modelling organismic movement at all scales.

10.2 Movement Ecology Meets Active Matter and Anomalous Dynamics

The approach that in the following we put forward for modelling the movements of organisms is based on cross-linking three fundamental fields of research. Briefly outlining them by focussing on important movement models used in these different research areas will set the scene for the precise formulation of our theory and its meaning in terms of the associated physical, mathematical and biological properties. We start with the most biological scientific field, moving down to more theoretical physical and mathematical formulations.

Movement ecology is a rather new discipline that endeavours to understand the movements of individual organisms, especially on larger scales, in view of interactions of the biological dynamics with the environment [25, 27]. While movement ecology is, to quite some extent, driven by experimental biologists [6, 7],

it has developed a mathematical framework in both statistical data analysis and probabilistic modelling by applying state space [28, 29], hidden Markov [28, 30] or random walk [26, 31] models to experimental data. For our approach, the concept of correlated random walks (CRWs) [32] developed within movement ecology is especially important. In two dimensions, this stochastic model describes the movement of an organism in terms of its step length, i.e. distance travelled per time step, and turning angle, both defined in a comoving frame [15, 31, 33]. Both variables are sampled independently and identically distributed at any time step from two associated probability distributions. In the simplest case, the step length may be chosen as constant while the turning angle is drawn from a non-uniform probability distribution, e.g. a Gaussian wrapped on the circle. Notably, the non-uniformity of the angular distribution models a persistence of the motion, i.e. a preference to move in the same direction, as is often observed in organismic movement, hence the notion of CRWs. Nevertheless, the whole stochastic process as defined above in the comoving frame is still Markovian, i.e. memoryless. CRWs have been widely applied to describe animal movement [31].

In contrast to movement ecology, the field of *active matter*, which developed in parallel over the past two decades, focusses on understanding the collective dynamics and the resulting material properties of a large number of interacting living agents at all scales, from swarms of bacteria to cytoskeleton gels in living cells, to schools of fish and flocking birds [16–18, 34]. Single entities of active matter can in turn be modelled as *active particles* [4, 14, 15, 35]. In detail, in contrast to the passive Brownian motion of a tracer particle in a fluid, which emerges from collisions with the surrounding fluid molecules, active biological motion is generated by an agent itself, due to taking up energy from the environment and converting it into self-propulsion [14, 15, 35]. This phenomenon is formulated mathematically most conveniently in terms of Langevin dynamics. For a passive Brownian particle in a fluid, the famous LE reads [36, 37]

$$m\dot{\mathbf{v}} = -\eta\mathbf{v} + \boldsymbol{\xi}(t), \tag{10.1}$$

with velocity $\mathbf{v} = \dot{\mathbf{x}}$ for a particle of mass m at position $\mathbf{x}$ at time t. The force on the right-hand side is decomposed into a viscous damping term with (Stokes) friction coefficient η while the random kicks of the microscopic surrounding particles are modelled by Gaussian white noise $\boldsymbol{\xi}$. Physically, this equation generalises Newton's second law to describing random-looking Brownian motion by decomposing the force into a deterministic and a stochastic component. Accordingly, the LE is sometimes called 'Newton's Law of stochastic physics'. Mathematically, it defines a stochastic differential equation generating an Ornstein–Uhlenbeck (OU) process for the velocity of the particle. The resulting Brownian motion is a Gaussian stochastic process characterised by a mean squared displacement that grows linearly in the long time limit, $\langle \boldsymbol{x}^2 \rangle \sim t$ $(t \to \infty)$, where the angular brackets denote an ensemble average, which yields what is called normal diffusion.

For modelling a self-propelled active particle, this LE has been modified in different ways. First, [14, 15, 35, 38], the constant friction η has been replaced by a speed-dependent friction coefficient,

$$m\dot{\mathbf{v}} = -\eta(s)\mathbf{v} + \boldsymbol{\xi}(t). \tag{10.2}$$

The simplest example is the linear Schienbein–Gruler friction defined by $\eta(s) = \eta_0(1 - s_0/s)$, where $s = |\mathbf{v}|$ denotes the speed of the particle, yielding $-\eta(s)\mathbf{v} = -\eta_0(s-s_0)\mathbf{e}_\mathbf{v}$ with $\mathbf{e}_\mathbf{v} = \mathbf{v}/s$ as the unit vector of the velocity. A non-linear version is the Rayleigh–Helmholtz friction, $\eta(s) = \eta_0(s^2/s_0^2-1)$, corresponding to $-\eta(s)\mathbf{v} = -\eta_0(s^2 - s_0^2)s\mathbf{e}_\mathbf{v}/s_0^2$ [14, 15]. The idea underlying this modification is that an active particle can take up energy from the environment by converting it into kinetic energy while it can also lose energy to the environment, depending on the sign of the friction term. Such an active particle aims at stabilising itself to move with a self-generated speed s_0 for which the active friction term is zero. This model has been called an *active Brownian particle* (ABP) in the original literature starting from the 1990s [15, 38].

A second type of active particle [4, 39] has been introduced by using an overdamped LE for which there is no particle acceleration anymore. Here the self-propulsion is achieved by a velocity term that is driven by angular noise,

$$\dot{x} = s_0 \cos\phi + \xi_x(t)\ ,\ \ \dot{y} = s_0 \sin\phi + \xi_y(t), \tag{10.3}$$

where ϕ is the polar angle of the (here and in the following two-dimensional) velocity vector $\boldsymbol{v} = (v_x, v_y)$ fixed at constant speed, s_0, and governed by rotational diffusion,

$$\dot{\phi} = \xi_\phi(t), \tag{10.4}$$

where ξ_ϕ is wrapped Gaussian white noise. That is, the orientation ϕ is generated by a Wiener process on the circle. This model has also been called an ABP in the literature, with some authors reserving this term for that particular model only [4].

A third generic type of active particle was also defined in terms of an overdamped LE [40, 41],

$$\dot{\mathbf{x}} = \mu_{\text{mob}}\boldsymbol{F}(\mathbf{x}) + \boldsymbol{\xi}_\text{c}(t)\ , \tag{10.5}$$

where $\boldsymbol{F}(\mathbf{x})$ holds for a force and μ_{mob} for the mobility of the particle. Here the Gaussian noise $\boldsymbol{\xi}_\text{c}$ is assumed to be coloured, typically in terms of exponential correlations [40],

$$\langle\boldsymbol{\xi}_\text{c}(0)\boldsymbol{\xi}_\text{c}(t)\rangle \sim \exp(-t/\tau), \tag{10.6}$$

which due to the non-Markovian memory yields active, persistent motion. In the case of a number of interacting active particles, the force is generated from a putative interaction potential [42]. If the exponentially correlated Gaussian noise is obtained from solving the OU equation (10.1) [41], this third model is called an active OU particle [42].

These three different models have in common that, inspired by the theory of passive Brownian motion, they are all formulated in terms of (underdamped or overdamped) generalised Langevin dynamics. However, in contrast to the LE (10.1) for a passive particle, they all model self-propulsion by including persistence that is very different from simple constant friction. In each of the three cases, the precise type of active persistence is entirely different. Furthermore, in all three cases, the fluctuation–dissipation relation is broken, as is typically found in active matter systems, since active particles operate far from equilibrium [16, 17]. On the other hand, in analogy to passive Brownian motion, all three types of active particle dynamics again exhibit normal diffusion in the long time limit, with the particles' persistence leading to an enhanced diffusion coefficient. On this basis, we classify all these three generic models of active particles that have been widely studied in the literature [4, 14, 15, 34, 35, 38–40] as ABP models, more specifically as ABPs type I, II and III, in (chronological) order of appearance.

Apart from this broad class of ABPs, there is another basic type of active particles describing run-and-tumble dynamics [43, 44]. For *Escherichia coli* bacteria under chemotaxis, it was observed [43] that these microswimmers perform sequences of long 'runs' in one direction, interrupted by periods of time where the bacteria 'tumble' by choosing a new direction, seemingly at random. This class of active motion can be modelled by using the overdamped LE (10.3) amended by the different equation for the dynamics of the polar angle ϕ [45]

$$\dot{\phi} = \Sigma_i \Delta\phi_i \delta(t - T_i) \,. \tag{10.7}$$

Here $\Delta\phi_i$ denotes the turning angle at times T_i when the particle tumbles, with both quantities drawn independently and identically distributed from a uniform distribution on the circle, respectively from some other (e.g. Poisson) distribution. In this particular sense, we have an ABP type IV with biological activity in terms of a specific tumble time distribution. However, there are other modelling approaches for run-and-tumble dynamics deviating from LEs [34, 40, 44]. We will not focus on run-and-tumble motion but will nevertheless come back to it in Sect. 10.4. This attempt of categorising active particle dynamics is of course not complete. There exist, for example, heterogeneous ABPs [46], anisotropic ABPs in three dimensions [47] as well as purely deterministic, nonlinear active particle models [48, 49] going beyond these four basic types.

At this point, there is already an important, although somewhat trivial, observation to be made. Namely, ABP II is intimately related to the CRW model of movement ecology introduced above in the sense that the self-propulsion term of ABP II, discretised in time, corresponds to a CRW model with a non-uniform wrapped Gaussian turning angle distribution. This is evident by noticing that the first terms in ABP II Eqs. (10.3), (10.4) represent the CRW model, defined within the comoving frame, transformed back to Cartesian coordinates by using time-continuous stochastic differential equations. Interestingly, ABP II is non-Markovian in the Cartesian frame, as the velocity autocorrelation function decays exponentially [50]. Hence, we have a Markovian representation of ABP II in the comoving

frame while there is a non-Markovian one in the Cartesian frame. We will come back to this interesting interplay between different frames of reference for defining stochastic processes in Sect. 10.4.

Mathematically, both movement ecology and active matter, the latter especially in view of ABPs, are rooted to quite some extent in stochastic theory, combined with statistical data analysis. In 1904, Sir Ronald Ross inspired [10] Karl Pearson to model the movements of organisms by a random walk in the plane, which led to a famous series of papers published by Pearson in 1905 and 1906 [11, 51]. Therein he defined a two-dimensional random walk in the comoving frame in complete analogy to setting up CRWs, with the only simplification that in addition to a constant step length, the turning angle is drawn from a uniform distribution on the circle. The paradigm of modelling biological movements as simple types of Brownian motion prevailed for almost a century. In parallel to the development of active matter theory, in the 1990s, this idea was questioned by experimental findings [19, 52] suggesting that albatrosses perform LWs characterised by *anomalous diffusion*, where in contrast to Brownian motion, the mean squared displacement increases nonlinearly with time, $\langle \boldsymbol{x}^2 \rangle \sim t^\alpha$ $(t \to \infty)$ with $\alpha \neq 1$. For the albatross, an exponent $\alpha > 1$ was found corresponding to superdiffusion; motion with $\alpha < 1$ is called subdiffusion [22–24, 37]. A two-dimensional LW can be easily formulated within the CRW framework by sampling the step lengths from an α-stable Lévy distribution [24] and assuming a uniform distribution of turning angles. As an additional constraint, the speed is held constant, thus inducing the very same power law distribution of corresponding flight times [53].

We remark that the hypothesis that organisms perform LWs is discussed controversially in the literature [19, 21, 54–57]. This relates to criticism of the underlying theory [21, 58] as well as to problems with the experimental data analysis, as it is difficult to argue for power laws when they stretch over a decade only and the methods of data analysis are not robust [55, 56]. On the other hand, this line of work indicates that biological dynamics may need to be described by stochastic processes that are more non-trivial than normal diffusive (active or passive) Brownian motion by exhibiting anomalous stochastic dynamics, thus going beyond the framework of both conventional movement ecology and active particles. Anomalous diffusion defines a very active field of research, mainly driven by mathematicians and theoretical physicists, who explore the diffusive properties of non-Markovian, non-Gaussian stochastic processes beyond Brownian motion [22–24, 37]. Such dynamics have been experimentally observed in a wide variety of real-world systems [20, 24]. Apart from Brownian motion and LWs, there are many other advanced stochastic models available for understanding biological movement, from intermittent processes where organisms switch between different modes of motion [59, 60] to other generic anomalous stochastic models like continuous-time random walks [61] or fractional Brownian motion [62]. More recently, anomalous diffusion has also been considered for modelling ABPs [63].

10.3 Data-Driven Construction of Generalised Langevin Equations for Modelling the Movements of Organisms

In the first part of this section, we will analyse movement data of three different types of organisms with the goal to construct generalised LEs in the Cartesian frame for them. We will first illustrate this approach for bumblebee flights by then applying it to cell migration and sea turtle foraging. Employing the very same theoretical framework, we will reveal non-trivial active and anomalous movement properties for these organisms. In the second part, bumblebee flights will be reconsidered by constructing from data an underdamped generalised LE in the comoving frame for them. We will show that this equation combines the characteristic features of the first three generic types of ABPs dynamics discussed in the previous section.

10.3.1 The Cartesian Frame

The very simple model that here we put forward for analysing movement data is the overdamped LE, obtained from the underdamped LE (10.1) in the limit of large friction where there is no particle acceleration anymore,

$$\dot{\mathbf{x}} = \boldsymbol{\xi}_{\mathrm{o}}(t) \,. \tag{10.8}$$

Here $\boldsymbol{\xi}_{\mathrm{o}}(t)$ denotes the noise of the overdamped equation. This model sits between time-discrete random walks and time-continuous underdamped LEs. A simple mathematical example is the Wiener process, for which the velocities are drawn from Gaussian white noise. As $\mathbf{v} = \dot{\mathbf{x}}$, in this equation, the distribution function of the noise $\rho(\boldsymbol{\xi}_{\mathrm{o}})$ matches to the velocity distribution function $\rho(\mathbf{v})$ of the moving organism, and the autocorrelation function of the noise $\langle \boldsymbol{\xi}_{\mathrm{o}}(0)\boldsymbol{\xi}_{\mathrm{o}}(t)\rangle$ is identical to the velocity autocorrelation function $\langle \mathbf{v}(0)\mathbf{v}(t)\rangle$ of the dynamics (here by assuming stationarity). Knowing both quantities fully defines this model, hence it can be constructed by extracting them from the data. This very elementary stochastic model, defined in the Cartesian frame, provides only a first approach and will be substantially refined in the next Sect. 10.3.2. In the following, we will nevertheless show that this simplistic framework can already yield a lot of insight into the origins of organismic movement. Most prominently featured by this model is the velocity autocorrelation function, which represents memory in the dynamics. An example is fractional Brownian motion, which can be generated by using for $\rho(\boldsymbol{\xi}_{\mathrm{o}})$ fractional (power law correlated) Gaussian noise [23, 62]. However, allowing arbitrary correlations obtained from data goes beyond other standard models such as Brownian motion, CRWs or LWs.

Starting from Eq. (10.8), we will first construct a stochastic model for bumblebee flights tracked in a laboratory experiment [64], as illustrated in Fig. 10.1(middle). A single bumblebee (*Bombus terrestris*) was flying in a cube of 75 cm side length

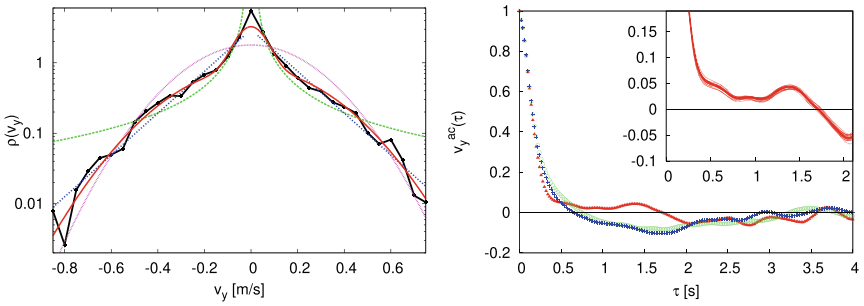

Fig. 10.2 Left: Semi-logarithmic plot of the velocity distribution $\rho(v_y)$ parallel to the y axis in the experimental set-up illustrated in Fig. 10.1(middle) (black crosses) for a single bumblebee in the spider-free phase (1). Included are lines for maximum likelihood fits with (from bottom to top in left corner) a single Gaussian (violet dotted), a Gaussian mixture (red line), an exponential (blue dotted) and a power law (green dashed). Right: Velocity autocorrelation function Eq. (10.9) for bumblebee velocities v_y in the three different phases of the experiment as described in the text: (1) red triangles, no spiders; (2) green circles, spiders; (3) blue crosses, spiders, memory test. The effect of the presence of spiders on the bumblebee flights is clearly seen, even in the memory test. The inset displays the resampled autocorrelation for stage (1) confirming that the positive autocorrelations are not a numerical artifact. Figures are from Ref. [2]

with a vertical grid of artificial yellow flowers on the wall in the back. Each flower was equipped with a landing platform and a source of nectar, replenished after consumption. The goal of the experiment was to analyse how bumblebee flights change under predation risk. For this purpose, four of the 16 flowers were randomly equipped with spider images, and 30 bumblebees were trained by a specific mechanism to avoid any flower with a spider image. The flight of a single bumblebee in this arena was recorded by two high frame rate (0.02 s) cameras yielding on average 6000 data points per bumblebee trajectory. In the following, we will analyse three phases of the experiment, which are (1) spider-free foraging; (2) foraging under predation risk; (3) a memory test with the same setting as (2) 1 day later; see Ref [64] for full details of the experiment.

First, we discuss the velocity distributions in phase (1) by focussing on $\rho(v_y)$ horizontally parallel to the wall, see the coordinate system in Fig. 10.1(middle), which turned out to be symmetric. The other ones along x and z were found to be asymmetric, due to the setup of the experiment or gravity, respectively. Applying maximum likelihood fits together with information criteria $\rho(v_y)$ shown in Fig. 10.2(left) was found to be best fitted by a mixture of two Gaussians representing two different flight modes, one with larger variance far away from the flowers and another one with smaller variance close to them, as confirmed by an additional spatial data analysis [2]. Hence, a bumblebee flies with on average smaller velocities when approaching a flower and with larger ones farther away from it. This corresponds to spatio-temporal intermittent motion, suitably adapted to this environment by exhibiting different flight modes when searching for food sources, respectively accessing them [59, 60].

Very surprisingly, the velocity distribution of phase (1) did not change in phases (2) and (3) under predation risk [2]. One might have expected that the bumblebees are getting more nervous in the presence of enemies, leading to flights with larger velocities, but this was not the case. Instead, the whole adaptation in the dynamics to environmental predation risk is contained in the velocity autocorrelation functions. Shown in Fig. 10.2(right) are the normalised velocity correlations horizontally parallel to the wall,

$$v_y^{\mathrm{ac}}(\tau) = \sigma^{-2} \left\langle (v_y(t) - \mu)(v_y(t+\tau) - \mu) \right\rangle_{\mathrm{e},t} , \tag{10.9}$$

where μ and σ^2 denote the mean and the variance of the corresponding velocity distribution of v_y, respectively, and the subscripts of the angular brackets denote a combined time-ensemble average over all bumblebees and over time. The time dependence of this quantity yields important information about persistence, memory and overall the topology of a bumblebee path. One can see that in the spider-free phase (1), the correlation decay remains positive for about 1.5 s representing persistence, that is, the bumblebee keeps flying in the same direction it came from. In contrast, for phases (2) and (3) under predation risk, the decay immediately becomes negative, which implies anti-persistence: The bumblebees quickly reverse the velocities by making more turns. This reflects the predation threat, as the flights are much less directed than in phase (1), i.e. more curvy, so the bumblebees are more careful. However, this change is only represented in the topology of the path, not in the velocity distributions, perhaps because the bumblebees find it more difficult to change their speeds.

In summary, after statistical analysis of experimental bumblebee data guided by Eq. (10.8), for an overdamped generalised LE modelling bumblebee flights under predation risk, the velocities are sampled from the mixture of two Gaussians identified by fitting the data in Fig. 10.2(left), correlated in time by using (suitably simplified versions of) the velocity autocorrelation functions shown in Fig. 10.2(right), depending on the phase one wishes to model. This stochastic model corresponds to a generalised version of ABP III Eq. (10.6), because the noise is non-trivially correlated, hence non-Markov and active. In addition the noise distribution is a bit more complicated than a simple Gaussian reflecting spatio-temporal intermittency. The coupling to the environment, in the spirit of movement ecology, can qualitatively be reproduced by another, related LE model, where changing the correlation function under predation risk is modelled by an interactive force term, as shown in Ref. [2]. A more refined model for bumblebee flights will be built in Sect. 10.3.2, therein defined fully analytically.

Along the same lines and again driven by experimental data analysis, an overdamped LE (10.8) can be constructed for cell chemotaxis [1]. Shown in Fig. 10.1(left) are the paths of 60 wild-type murine neutrophil cells recorded over $T = 30$ min with a sampling interval of 5 s yielding 361 data points per track. For these cells, the velocity distributions were found to be simple Gaussians [1]. Figure 10.3(top) displays the associated velocity autocorrelation functions, here

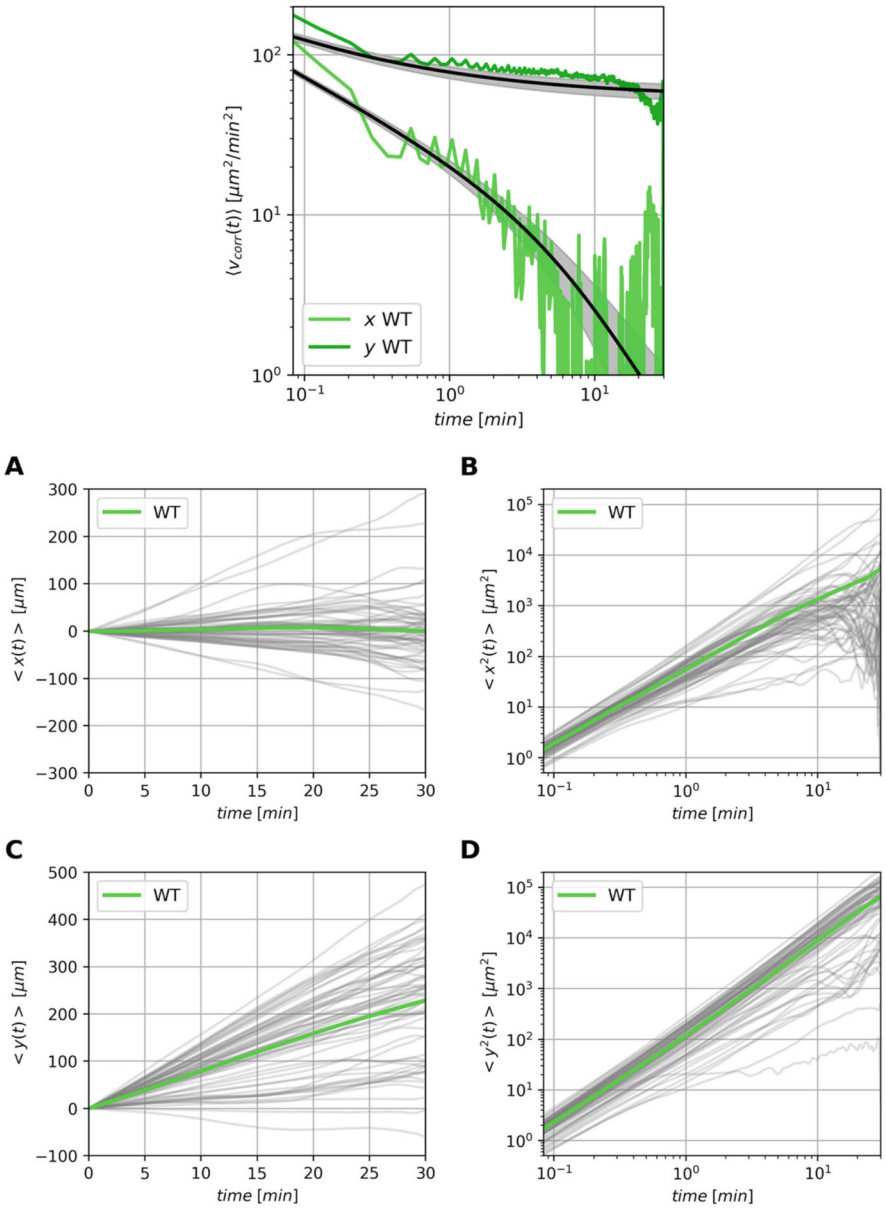

Fig. 10.3 Top: Velocity autocorrelation functions along x and y for wild-type neutrophils performing chemotaxis parallel to the y-axis. Thick green lines show the combined time-ensemble averaged correlation function obtained from data for the x and y direction in bright and dark colors, respectively. The fits discussed in the text are included as bold black lines together with a grey area of uncertainty ($\pm$ one standard deviation). Bottom: Corresponding first and second moments of positions along x and y. Thin grey lines show time-averaged moments of single cells. Thick green lines display the combined time-ensemble average of the corresponding moment. Figures are from Ref. [1]

denoted by $\langle v_{\rm corr}(t)\rangle$, defined again by a combined time and ensemble average but not normalised and without subtracting the drift. The fits represent, along y, pure power law correlation decay, $\langle \xi_y(t)\xi_y(t')\rangle \sim \tau^{2H-2}, \tau = |t-t'|, 0 < H < 1$, and along x the same with power law tempering, $\langle \xi_x(t)\xi_x(t')\rangle \sim \tau^{2H-2}(1+\tau/\tau^*)^{-\mu}, \mu, \tau^* \geq 0$. However, as Fig. 10.1(left) indicates, here we have motion with an average non-zero drift along the chemical gradient in the y direction, which deserves further analysis. Fig. 10.3(bottom), showing first and second moments of the position distributions along x and y as functions of time, demonstrates that indeed there is a drift linear in time along y with $v_{\rm d} \simeq 7.4\,\mu$m/min while there is no drift along the x direction perpendicular to the chemical gradient. These results suggest a modelling of this cell chemotaxis in terms of the generalised overdamped LE

$$\dot{x} = \xi_x(t), \;\; \dot{y} = v_{\rm d} + \xi_y(t). \tag{10.10}$$

The dynamics along y represents (biased) fractional Brownian motion [23, 62]. Along the x-axis, there is no drift, but the correlations are power law tempered. These results reflect the symmetry breaking by the chemical gradient and long-term persistence induced by it. Accordingly, this dynamics yields anomalous (super) diffusion both along x and y as shown in Fig. 10.3(bottom) by the second moment obtained from the data, with exponents α changing between 1.2 and 1.5 along x, due to the tempering, and $\alpha \sim 1.55$ along y. Note that the associated (anomalous) diffusion coefficients, i.e. the prefactors in the mean squared displacement, are more than an order of magnitude larger along y than along x yielding a much faster diffusion parallel to the gradient. The same analysis has been performed for three other cell types that have been chemically modified, revealing subtly different chemotactic dynamics in terms of the resulting LEs, which helps to understand the impact of specific chemical modifications on chemotaxis, as well as identifying cell deficiencies [1].

In summary, for neutrophil cells we have constructed a generalised overdamped LE from data that again may be associated with ABP III, as the noise is non-trivially correlated; hence, the dynamics is again non-Markovian and active, though Gaussian. In contrast to the previous bumblebee model, however, these cells display anomalous (super) diffusion, which demonstrates the need to go beyond Markovian normal diffusive Brownian motion models to understand organismic movement [13, 65, 66].

Finally, as a third example of data-driven application of the overdamped LE framework based on Eq. (10.8), we present results for the off-shore foraging of loggerhead sea turtles *(Caretta caretta)*. A sample path is depicted in Fig. 10.1(right). These turtles are listed as endangered on the IUCN red list; hence, learning about their foraging activities is important for improving their protection. The length of a typical loggerhead sea turtle in this population of Cabo Verde is around 75–85 cm of carapace. The largest individuals can weight up to 135 kg and some may live

up tp 60 years in the wild. If threatened, in short burst, they can swim up to 35 km/h. The group of turtles studied in this experiment [67] nested on the Cabo Verde islands from which they swim in directed paths to the coastline of West Africa, where they forage. For this experiment, 23 turtles have been tagged since 2011 using satellite-relayed ARGOS systems so that their positions could be recorded at high accuracy [67]. The following results [9] are for a female turtle named Mokamba, where around 1350 data points have been obtained over 400 days from August 2012 to September 2013.

A crucial difference to the previous two organisms, whose positions have been determined with high constant frame rates in a lab, is that these turtles have been tracked via satellites in the wild. As signals could only be emitted with different quality when a turtle was close to the surface, and sometimes the satellite was not available to receive the signal, all turtle data are recorded with varying precision and at irregular time intervals. This poses a severe problem to any reliable statistical data analysis. First, the turtle data had to be cleaned by a specific procedure for removing, e.g. unrealistic or duplicate data points. Then the data had to be interpolated, as statistical averages can only be constructed based on data sets sampled at constant time intervals. Here we chose the most straightforward way of linear interpolation by resampling the interpolated data with a constant time interval, given by the average of the underlying irregular time intervals; details of the full data analysis are given in Ref. [9].

First, we extracted the velocity distributions from the data in a Cartesian coordinate system aligned to longitude and latitude, where according to Fig. 10.1(right) the y-axis is on average almost parallel to the coastline. It was found that both velocity distributions are best fitted by symmetric Gaussians for small velocities while they showed exponential tails for large velocities, in combination matching well to a Gamma distribution, related to what was reported for albatross flights [55]. No significant deviations between velocities along x and y were detected in the data. This corresponds to spatio-temporal intermittency in the turtle movements as an alternation between two different movement modes, similar to our previous results for bumblebee flights. However, here the intermittency occurs as a random-looking switching between foraging (diving, searching, small velocities) and travelling to the next foraging spot (larger velocities). Most interesting were, again, the velocity autocorrelation functions, computed by time averaging along the trajectory. The one for v_x is shown in Fig. 10.4(left); the one for v_y looks similar, but the oscillations are a bit more irregular. Both correlation functions are best fitted by the functional form $\langle v_x(0)v_x(t)\rangle_t = a\exp(-bt) + c\cos(dt)$, where a, b, c, d are fit parameters. This corresponds to exponential decay for very short times while the long-time dynamics exhibits persistent oscillations with a certain period. Figure 10.4(right) displays the corresponding mean squared displacement $\langle x^2(t)\rangle_t$ computed from the data, again via time averaging. One can see that on time scales up to 100–200 h, the turtle moves superdiffusively with an exponent of approximately $\alpha \simeq 1.7$ while for longer times the graph crosses over to subdiffusion, eventually leading to localisation.

Based on these experimental findings, we simulated an overdamped LE where the noise was sampled from a Gaussian (ignoring the exponential tails) with the

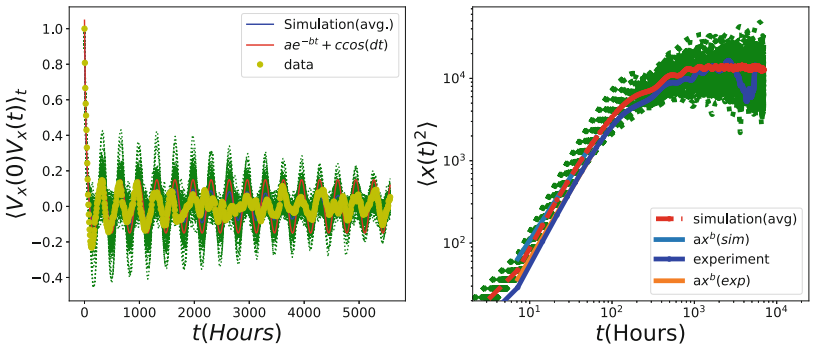

Fig. 10.4 Left: Velocity autocorrelation function along x for a loggerhead sea turtle foraging off the coast of West Africa. The filled olive circles show experimental data, the thin red line with constant oscillation amplitude our best fit to this data, the green dots results from individual simulations of our stochastic model and the blue line with varying amplitude the ensemble averaged simulation result. Right: Corresponding mean squared displacement along x. The wiggled blue line shows experimental data, the overlapping straight orange line is a power law fit to the data for short times, the green dots result from individual simulations of our stochastic model, the (mostly hidden) dashed red line depicts our ensemble averaged simulation result and the turquois line matching the red line at short times yields a power law fit to the simulation results. Figures are from Ref. [9]

correlation decay as identified above, amended by boundary conditions. One can observe in Fig. 10.1(right) that the turtle swimming is bounded from the right by the continental shelve, and on the left, there is also some less rigorous boundedness, likely associated with deeper and less productive (food-rich) waters. We modelled this qualitatively by adding to the LE a force generated by a harmonic potential with slightly asymmetric prefactors to the left and to the right. The numerical results are compared to the experimental data in Fig. 10.4 showing excellent agreement. What one can learn from this stochastic model is that, first, again there is biological activity along the lines of ABP III, as the noise is non-Markovian correlated. Second, the turtles move superdiffusively for shorter times. This is directly related to the strong, very slow periodic oscillations seen in the correlation function: the average half period of one oscillation is about 200 h and thus matches approximately to the cross-over time to subdiffusion seen in the mean squared displacement. Hence, the turtle swims in a rather directed way superdiffusively before it turns around due to hitting the boundaries of the chosen foraging region, which induces subdiffusion (eventually crossing over to localisation on longer time scales; not seen here but for other turtles [9]). The average distance swam during 200 h calculated from the mean squared displacement is approximately 83 km. This matches in order of magnitude to the longitudinal width of the turtles' foraging region, which is hard to estimate but lies around 100–200 km. All these details explain the large scale 'looping' seen in the trajectory displayed in Fig. 10.1(right). That the oscillations in the velocity autocorrelations do not decay may be considered as an unusually strong sign of biological activity. One might speculate that the turtles have developed this looping

as an optimal foraging strategy to efficiently search this region. It was checked that the looping is not generated by ocean currents, nor do the turtles exhibit chirality, as often observed for microswimmers [4]. However, there is some coupling to the chlorophyll concentration that is a proxy for food sources, which is ignored in this modelling.

To summarise this section, we have applied the rather basic approach of a generalised overdamped LE to explain the experimentally recorded movements of three very different types of organisms. In all three cases, the stochastic model constructed from data showed that the most significant information is not contained in the associated probability distributions, which is in sharp contrast to the optimal foraging hypothesis based on LWs [19]. Instead, important details characterising the biological movements are captured by the velocity autocorrelation function. That these quantities deserve more attention when analysing movement data has already been emphasised in Ref. [2]. In all three cases, the observed dynamics turned out to be non-Markovian correlated, which may be understood as biological activity along the lines of ABP III. In two cases, the associated diffusion was furthermore anomalous. The constructed models were also to some extent capable to reproduce couplings with the environment in the spirit of movement ecology.

While this straightforward approach of stochastic model building seems to be very promising for further experimental data analysis of organismic movement by already providing significant insight into the emergence of the observed biological dynamics, it is theoretically somewhat a bit naive. In the next part, we will show that one can do much better by drawing inspiration from movement ecology, which suggests to analyse data in the comoving frame.

10.3.2 The Comoving Frame

The CRW model of movement ecology introduced in Sect. 10.2 entails to analyse movement data in a frame attached to the centre of mass of an organism cotranslating and corotating with its movements, which we call the *comoving frame*. This frame is biologically very well motivated, as it seems natural to think of higher-dimensional movements of organisms in terms of step length and turning angle. On the other hand, while a CRW already exhibits persistence, as discussed in Sect. 10.2, it still belongs to the simple class of Markovian overdamped random walks and thus looks somewhat artificial in order to capture the full spectrum of organismic movement. For that reason, in Ref. [33], the conventional CRW model was generalised by formulating underdamped non-Markovian dynamics in a comoving frame. Inspiration was taken from underdamped Langevin dynamics, see Eq. (10.1), which suggested to write down ad hoc the following two Langevin-type equations of motion in the comoving frame:

$$\dot{\beta} = h(\beta, s) + \xi_{\beta;s}(t), \tag{10.11}$$

$$\dot{s} = g(\beta, s) + \xi_{s;\beta}(t). \tag{10.12}$$

In the spirit of a CRW, here β denotes the *turning angle* defined by integration over the angular velocity of the orientation ϕ, $\beta(t) = \int_{t-\Delta t}^{t} \dot{\phi} dt$ [33]. Note that ϕ refers to the polar angle of the velocity vector $\mathbf{v}$ of the moving organism defined in the Cartesian frame, as introduced in Eq. (10.3). Likewise, s holds for the speed of the moving organism, i.e. the radial component of the velocity in the Cartesian frame, cf. Eq. (10.2). In summary, Eqs. (10.11), (10.12) are based on an interplay between three different coordinate frames: (1) The usual fixed Cartesian frame in which overall the three ABP models of Sect. 10.2 were defined; (2) the polar frame in which the speed of ABP I [15] and the velocity of ABP II were defined; and (3) the comoving frame, which refers to a *self-consistent* definition of the dynamics of a moving agent in terms of the turning angle β and its speed s only, i.e. without any explicit reference to the Cartesian or polar frames (1) or (2). Examples of such dynamics are the CRW of movement ecology and the Langevin-type equations introduced above. The tricky part, crucially distinguishing the comoving from the polar frame, is to obtain a self-consistent equation for the turning angle variable, as for the example of the OU process we will show in Sect. 10.4.

To conclude the discussion of the new model Eqs. (10.11), (10.12), both equations are underdamped featuring acceleration of β and s on the left-hand side, which is generated by splitting the dynamics into deterministic drift and stochastic diffusion terms on the right-hand side. While this very basic structure corresponds to the one of the ordinary LE (10.1), here the functional forms of these four terms, including the autocorrelation decay of the two noises, are per se completely general and need to be determined, e.g. by experimental data analysis. For this reason, we use the more general notation $h(\beta, s)$ and $g(\beta, s)$ for the drift terms, even though at least for the speed, we would expect the respective term to boil down to some type of friction, cf. $\eta(s)$ in ABP I Eq. (10.2), as indeed will be shown in the following.

We now demonstrate that Eqs. (10.11), (10.12) can be used to analyse movement data by standard methods of drift-diffusion time series analysis. As an example, we construct a stochastic model for 'free' bumblebee flights by applying this framework to the experimental data discussed in Sect. 10.3.1, where here we only consider flights far away from the flower carpet in the spider-free phase (1). The analysis was based on 51 trajectories with approximately 49,000 data points [33]. Plotting the normalised drift vector field of (s, β), respectively the deterministic terms of Eqs. (10.11), (10.12) extracted from data, shows that the cross-dependencies of $h(\beta, s)$ on s and of $g(\beta, s)$ on β are weak [33]. This suggests to split the vector field into

$$\dot{\beta} = h(\beta) + \xi_{\beta;s}(t), \tag{10.13}$$

$$\dot{s} = g(s) + \xi_{s;\beta}(t). \tag{10.14}$$

Figure 10.5 depicts results for both simplified drift terms, extracted from data and with fits to the data. As can be seen in Fig. 10.5(top), $h(\beta) \simeq -k\beta$ with $k \approx 1/\Delta t$.

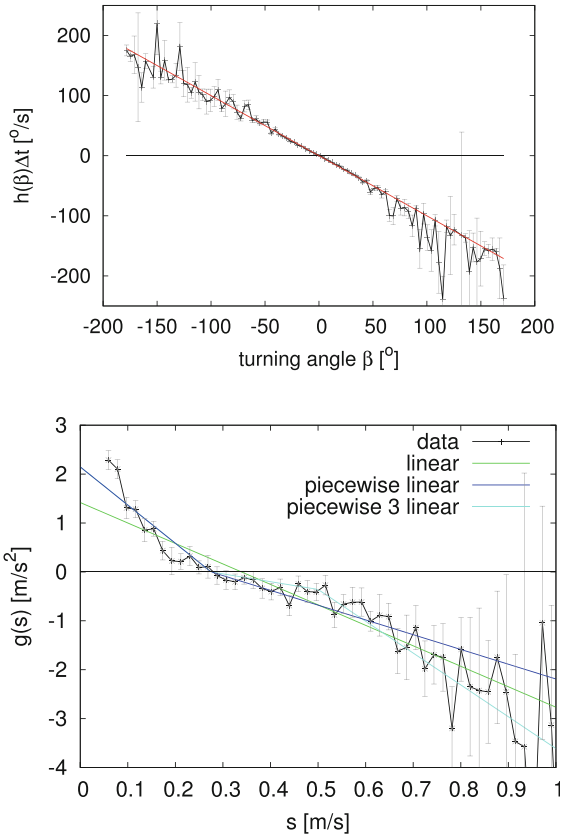

Fig. 10.5 Top: Drift coefficient for the turning angle β. The drift $h(\beta)$ obtained from bumblebee data (wiggled black line) is linear in β, as demonstrated by the fitted straight red line. Bottom: Drift coefficient for the speed s. Here the drift $g(s)$ obtained from bumblebee data (black wiggled line) has been approximated by piecewise linear functions from one to three pieces (blue, green, cyan, right corner from top to bottom). 95% confidence intervals are shown in grey. Figures are from Ref. [33]

Integrating Eq. (10.13) with respect to Δt yields $\beta(t) = \tilde{\xi}_{\beta;s}(t)$ [33]. Hence, for the angular dynamics, we are almost back to a CRW where the turning angles are sampled from some probability distribution, except that here we allow them to be correlated both with respect to s and in time. Determining analogously the drift term $g(s)$ in the speed equation (10.14) from data suggests simple (piecewise) linear approximations as suitable fit functions, cf. Fig. 10.5(bottom). For an analytical model, we choose the one consisting of two pieces,

$$g(s) \approx (s - s_0) \cdot \begin{cases} -\eta_1, s < s_0, \\ -\eta_2, s \geq s_0, \end{cases} \tag{10.15}$$

with $\eta_1 > \eta_2 > 0$ and a preferred speed s_0. We see that this deterministic drift term constructed from data yields an expression that, interestingly, can be understood as an active, speed-dependent friction coefficient, which is somewhat in-between the Schienbein–Gruler and Rayleigh–Helmholtz forms discussed for $\eta(s)$ in ABP I, Eq. (10.2).

We now take on the two noise terms in Eqs. (10.11), (10.12). First, it was found that the turning angle distribution $\rho_s(\beta)$ at each speed is best approximated by a wrapped Gaussian [33]. However, the standard deviation σ_β turned out to be strongly speed-dependent, with exponential decay in s fitting best [33]. This matches to naive biological reasoning: At larger speeds, it is more difficult for a bumblebee to make frequent turns. It remains to determine the correlation decay of the turning angle dynamics, where the autocorrelation function is defined in analogy to Eq. (10.9). Figure 10.6(top) shows that it follows a steep power law. This analysis yields a stochastic process for the turning angle dynamics defined by

$$\beta = \tilde{\xi}_{\beta;s}(t),\ \tilde{\xi}_{\beta;s} \overset{d}{\sim} \mathcal{N}(0, \sigma_\beta(s)),\ \sigma_\beta(s) = c_1 e^{-c_2 s} + c_3, \tag{10.16}$$

with c_1, c_2, c_3 as fit parameters, where the turning angle noise is power law correlated.

Second, the noise for the speed changes can be computed from Eq. (10.12), rewritten as $\xi_{s;\beta}(t) = \dot{s} - g(s)$. This noise obtained from data showed no dependence on β and was best fitted with a Gaussian [33]. The correlations, defined in the same way as in Eq. (10.9), turned out to be anti-persistent, as depicted in Fig. 10.6(bottom), which was best approximated by a difference between two exponential terms, $\mathrm{acf}_{\xi_s}(\tau) \approx a e^{-\lambda_1 \tau} + (1-a) e^{-\lambda_2 \tau}$, $\lambda_1, \lambda_2 > 0$. This completes Eq. (10.14) for the speed dynamics.

In summary, we obtain as a full stochastic bumblebee flight model

$$\beta = \tilde{\xi}_{\beta;s}(t), \tag{10.17}$$

$$\dot{s} = -\eta_i (s - s_0) + \xi_s(t),\ i = 1, 2, \tag{10.18}$$

where $\tilde{\xi}_{\beta;s}$ is speed-dependent, power law correlated wrapped Gaussian noise defining the turning angle β at each time t. The speed dynamics is governed by an underdamped LE with a speed-dependent piecewise linear friction coefficient and exponentially anti-correlated Gaussian noise ξ_s. As shown in detail in Ref. [33], this fully analytically defined model, which is based on quite some approximations, works surprisingly well to reproduce the experimental bumblebee flight data it was constructed from.

There are some important conclusions to be drawn from this part, which we summarise as follows. We have shown that starting from the (underdamped) generalised LE (10.11), (10.12) formulated in the comoving frame for both the turning angle and the speed dynamics, one can construct a corresponding stochastic model from data for 'free' (modulo the experimental setup of the cage) bumblebee flights. Interestingly, the speed equation contains a speed-dependent friction term right in the spirit of ABP I. The angular dynamics features a wrapped Gaussian turning angle distribution as for a standard CRW and the associated ABP II. Finally, both the angular and the speed dynamics exhibit correlated, non-Markovian noise

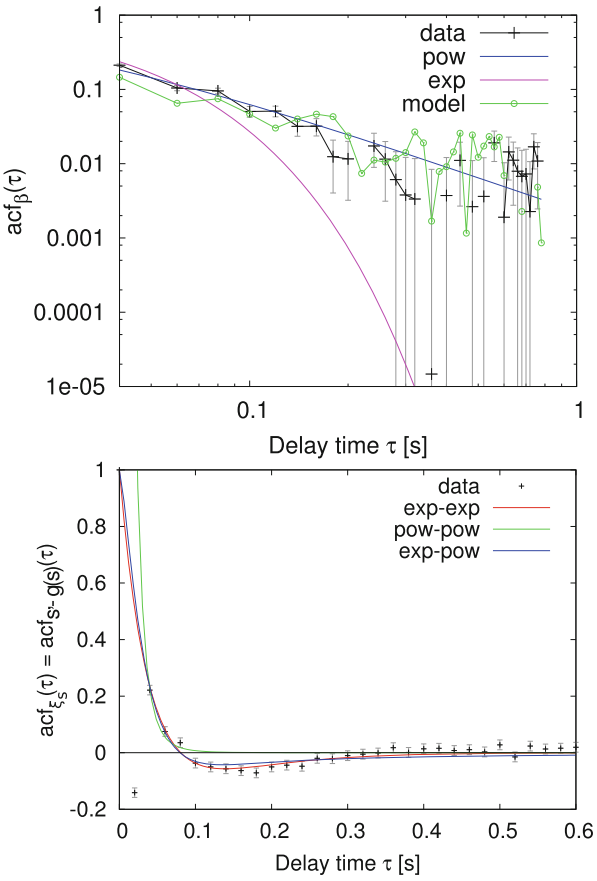

Fig. 10.6 Top: Autocorrelation function for turning angles β. Experimental data (black crosses) is shown together with an exponential (magenta curved line) and a power law (blue straight line) fit, supplemented by the large-lag standard error (grey). The green circles depict the autocorrelation extracted from the simulated data Eqs. (10.17), (10.18). Bottom: Autocorrelation of the non-deterministic speed changes ξ_s from experimental data (dots) with two times the large-lag standard error (grey) and three fits (top left corner left to right): Difference of two exponentials (red), exponential and power law (blue) and of two power laws (green). The outlier at $t \sim 0.02$ s is a discretisation artefact due to the finite resolution of the data. Figures are from Ref. [33]

terms, thus displaying the main property of ABP III. We have thus constructed from experimental data a movement model for bumblebee flights that contains the characteristic features of all three generic ABP models I–III discussed before. When Ref. [33] was published in 2013, only activity related to ABP I was pointed out but not the cross-links to ABP II (invented earlier) and III (invented later), with the field of active particles still being in rapid development during that time. Whether this model generates anomalous diffusion was not tested. There is no mechanism for such dynamics in the Gaussian noise distributions, but the turning angle correlations decay as a power law, similar to the fractional Brownian motion stochastic model for the angular dynamics studied in [63]. Therein it was shown, however, that such dynamics only displays transient, no long-term anomalous diffusion. More general conclusions based on this analysis are drawn in the following section.

10.4 A Newtonian Equation for Modelling the Movements of Organisms

How do you, reader, walk in a plane? You make a step per time interval by choosing a direction and a step length, and you repeat the process. Typically, you include some memory for steering where you want to go. But this dynamics is per se generated by yourself solely in the comoving frame. Of course, you may wish to navigate, given environmental conditions (moving in a room full of objects, going shopping, etc.). But we do not compute our intrinsic movements in a fixed Cartesian frame by then translating these results into the active movement outlined above, nor is there any reason why other living organisms should do so. Representing passive, environmentally generated movement mathematically in a fixed Cartesian frame makes perfect sense for modelling physical phenomena like Brownian motion of a tracer particle in a fluid, where the fluid is contained in some region and the tracer is driven passively by the surrounding fluid molecules. However, any living organism is self-propelled by 'biological noise' *internally* generated by the organism itself, *and thus in the comoving frame*, not originating *externally* in some fixed Cartesian frame. The latter should rather model external environmental noise on top of internal biological activity. For these biophysical reasons, we argue that the right frame to work in for understanding the movements of organisms is primarily the comoving one, not the fixed Cartesian one. This was already amply realised by Sir Ronald Ross in 1904 when he suggested to Karl Pearson to model mosquito flights by using step lengths and turning angles. Pearson rephrased this idea in his 1905 papers in terms of the 'drunken sailor problem', where he defined the random walk of a drunken sailor in the comoving frame, not in the Cartesian one [51]. In that sense, the CRW formulated within movement ecology is a straightforward generalisation of Ross' and Pearson's ideas to a sailor who is not fully drunk by exhibiting some persistence. In contrast, the physically and mathematically inspired approaches of active particles and anomalous diffusion naturally use the Cartesian frame, reflecting their origin of describing passive motion and that stochastic processes are defined and analysed way easier in these coordinates. Accordingly, higher-dimensional formulations typically consist of straightforward component-wise vectorial extensions of one-dimensional stochastic processes in a Cartesian frame. Note also that, as we remarked in Sect. 10.2, a CRW can be formulated as a Markov process in the comoving frame while it exhibits non-Markovian properties in the Cartesian frame. To what extent this applies to other stochastic processes is an interesting open question, possibly also of some biological relevance.

The problem of representing stochastic processes in different frames of reference is exemplified by a recent experiment, whose aim was to synthetically generate different types of anomalous diffusion. For this purpose, the dynamics of a super-paramagnetic colloidal particle was finely tuned by using magnetic fields. These fields were changed in time according to specific protocols defined in the comoving frame, which were designed to reproduce generic types of anomalous diffusion [68]. This experimental approach raised the question of how to define anomalous

stochastic processes like LWs and fractional Brownian motion in the comoving frame. For LWs, the answer is to quite some extent known but, interestingly, ambiguous: In Ref. [53], it was shown that there exist three different LW models in two dimensions, two defined in the Cartesian frame and one in the comoving frame. What we introduced as LWs in Sect. 10.2 is actually only the version in the comoving frame, called uniform LW. It turns out that all three LW models exhibit different diffusive properties [53]; hence, they cannot be transformed into each other. This is due to the non-Markovianity of the LW dynamics. For other processes, such as two-dimensional Cartesian fractional Brownian motion, so far no corresponding formulation in the comoving frame is known; one may doubt whether there is any exact one, given the inherent non-Markovianity of this process.

The above discussion suggests that working in different reference frames requires very different definitions of stochastic processes. This problem has been solved for the Markovian OU process [69], defined in Eq. (10.1) for the velocity in the Cartesian frame (where in the following, we explicitly spell out the noise strength as $\sqrt{2D}$ with velocity diffusion coefficient D). Transforming the Cartesian OU process into the comoving frame requires to use polar coordinates for the velocities, as in ABP II Eq. (10.3), i.e. $v_x = s\cos\phi$, $v_y = s\sin\phi$. However, since both the associated speed s and the orientation ϕ are stochastic variables, we encounter an Itô-Stratonovich problem for defining the corresponding stochastic equations in the comoving frame. The Itô equations for (ϕ, s) were already derived in Ref. [70],

$$\dot{\phi} = \frac{1}{s}\sqrt{2D}\xi_\phi(t), \tag{10.19}$$

$$\dot{s} = \left(-\frac{\eta}{m}s + \frac{D}{s}\right) + \sqrt{2D}\xi_s(t), \tag{10.20}$$

with the two noises defined as

$$\xi_\phi(t) = -\xi_x(t)\sin\phi + \xi_y(t)\cos\phi,\ \xi_s(t) = \xi_x(t)\cos\phi + \xi_y(t)\sin\phi, \tag{10.21}$$

where ξ_x, ξ_y are the two corresponding Gaussian white noises in the Cartesian frame. One can show that the resulting two noises ξ_ϕ, ξ_s are also white Gaussian [70]. Equations (10.19), (10.20) can be solved numerically, confirming that they reproduce Cartesian OU dynamics [69]. However, in order to obtain a self-consistent description of OU in the comoving frame, we need an equation for the turning angle β. This can be accomplished starting from $\beta \simeq \dot{\phi}\delta t$ and by calculating the functional form of the turning angle distribution from the right-hand side of Eq. (10.19). One can show that in a steady state, the speed generated by Eq. (10.20) is distributed according to a Rayleigh distribution with exponentially decaying autocorrelations. Remarkably, the wrapping onto the circle entailed in the calculation yields turning angles that are uncorrelated. Hence, this wrapping, which is a crucial operation to generate self-consistent angular dynamics in the comoving frame, marks a highly non-trivial step of loss of memory. Along these lines one finds for the turning angle distribution

$$\rho(\beta) = \frac{\sqrt{2D\delta t}}{2\pi} \sum_{k=-\infty}^{\infty} \frac{\sigma_{\xi,\phi}\,|k|}{\sigma_{\rho,s}} K_1\left(\frac{\sqrt{2D\delta t}\;\sigma_{\xi,\phi}\,|k|}{\sigma_{\rho,s}}\right) e^{ik\beta}, \tag{10.22}$$

with $\sigma_{\xi,\phi}$ the standard deviation of the Gaussian noise ξ_ϕ in Eq. (10.19) and $\sigma_{\rho,s}$ the one of the Rayleigh distribution for the speed obtained from solving Eq. (10.20), where $K_1(z)$ is the modified Bessel function of the second kind. $\rho(\beta)$ looks overall similar to a wrapped Gaussian, respectively a von Mises distribution, but shows deviations in detail [69]. One thus arrives at a self-consistent formulation of a Cartesian OU process transformed into the comoving frame in the form of [69]

$$\beta = \xi_\beta(t),\ s = \tilde{\xi}_s(t), \tag{10.23}$$

where ξ_β is white noise with the functional form of $\rho(\beta)$ while $\tilde{\xi}_s$ is exponentially correlated Rayleigh noise. Alternatively, the equation for the speed could be replaced by Eq. (10.20) with Gaussian white noise for ξ_s.

In summary, in this section, we first argued that for biophysical reasons, organismic movement models should ideally generically be defined in the comoving frame. We then demonstrated that this change of perspective has profound implications on the corresponding description of movement in terms of stochastic processes. While a Markovian OU process can still be transformed exactly from the Cartesian into the comoving frame, this is not possible anymore for non-Markovian LWs and appears unlikely for other non-Markovian processes like fractional Brownian motion. The resulting Eqs. (10.23) for OU in the comoving frame illustrate the framework provided by Eqs. (10.11), (10.12), which define generalised Langevin dynamics in the comoving frame. Equations (10.17), (10.18), on the other hand, demonstrated that a comoving generalised LE can also be constructed from experimental data. Similarly, this theoretical framework contains CRWs and LWs as special cases by furthermore capturing all characteristic features of ABP I–III. It also includes run-and-tumble dynamics if described by what we called ABP IV. These findings substantiate the purely heuristic formulation of Eqs. (10.11), (10.12) as a promising candidate for what one may call a Newtonian equation for modelling the movements of organisms, in the form of a generalised LE in the comoving frame.

This theoretical framework raises some important open questions. First, both the bumblebee model and the OU process in the comoving frame yield turning angle dynamics that does not involve a first-order time derivative as proposed in the original Eq. (10.11). Upon further scrutiny, one may argue that such a first-order differential equation for the turning angle models a kind of 'jerky' angular acceleration that goes beyond classical Newtonian dynamics. At present, it is not clear whether such a higher-order modelling is needed for describing biological movements, or not. On the other hand, there is no reason why organismic movement should obey simple Newtonian-type dynamics. Second, OU dynamics in the comoving frame is represented by a non-uniform turning angle distribution that reminds of ABP II as well as by exponential speed correlations similar to APB III. Hence, one may question whether characterising biological activity based on the existence

of non-uniform turning angle distributions or correlations only is sufficient, as these properties also characterise passive OU dynamics transformed into the comoving frame. This asks for a more robust, general classification of active biological motion. Along these lines, third, OU for a passive particle exhibits fluctuation–dissipation relations while for an active particle, they are typically expected to be broken. It is not clear, however, how fluctuation–dissipation relations look like for dynamics in a comoving frame. These appear to be important theoretical questions that require further investigation.

10.5 Conclusions

The LE provides a powerful paradigm, which has been widely used across different fields of science. Originally formulated to model the Brownian motion of a tracer in a fluid, this concept has been successfully applied in terms of geometric Brownian motion to economics and, more recently, to climate science for modelling the temperature of the Earth [71]. Here we argue that it may be similarly promising to apply a suitably generalised LE for modelling and understanding the movements of organisms. In order to do so, we combined key concepts and ideas extracted from movement ecology, active matter and anomalous diffusion. We first demonstrated that a very simplistic application of Langevin dynamics in terms of a generalised overdamped LE formulated in the Cartesian frame already proves useful to describe experimental results for foraging bumblebees, migrating cells and swimming sea turtles. In all these cases, the resulting LEs constructed from data contained specific features of ABPs, partially together with properties of anomalous diffusion. We then showed that a more general, and biophysically more meaningful, formulation of generalised Langevin dynamics can be achieved by using the comoving frame. Working out this idea for bumblebee flights we constructed a generalised underdamped LE from data in the comoving frame, combining the characteristic features of all three ABP models discussed before. We also outlined an application of this framework to a recent experiment synthetically generating anomalous diffusion. Theoretically, we illustrated this formalism by transforming the Markovian OU process defined in the Cartesian frame into a new set of stochastic equations defined self-consistently in the comoving frame. Whether the transformation of known stochastic processes from the Cartesian into the comoving frame is generally the right way to study organismic movement may be questioned. Rather, it looks as if this theoretical framework asks for a formulation, and study, of novel stochastic processes specifically defined in the comoving frame. Our central result is the generalised LE in the comoving frame Eqs. (10.11), (10.12), already put forward in Ref. [33], which we advertise as a promising approach to model the movements of organisms. This equation asks to be tested experimentally for movements of other organisms and laboratory-based studies with synthetic active matter (e.g., active colloids [68]). Such experiments can help to identify and formulate generic, potentially new stochastic processes for

explaining other observed dynamics. The proposed theoretical framework, in turn, poses interesting new mathematical problems in terms of formulating stochastic processes in the comoving frame by studying their statistical physical properties.

In view of a biological meaning, the theory that we put forward here may relate in some sense to the work by Uexküll [72]. Along similar lines, the Cartesian and the comoving frames that we identified as being intimately associated with different representations of stochastic dynamics for modelling organismic movement may have direct biological interpretations in terms of what is called allocentric and egocentric reference frames [73]. The interplay between these two frames is in turn very important for understanding organismic navigation strategies like path integration [73, 74]. Interestingly, recent research provides evidence that these two different, biologically highly relevant frames are linked on a neural level in the brain of organisms to specific neurons called place and grid cells [74].

Finally, apart from movement ecology, active matter and anomalous diffusion, strictly speaking, another fourth research area comes into play within this framework, which is *nonlinear dynamics*. This is most easily seen in the ABP model I, which employs potentially nonlinear friction coefficients. More recently, there have been speculations about the origin of specific organismic movement patterns by nonlinear oscillatory dynamics in the brain [75, 76]. Along all these lines, the door seems wide open for new research to model and understand the movements of organisms from first principles.

Acknowledgments R.K. wishes to thank Friedrich Lenz, Aleksei Chechkin, Thomas Ings and Lars Chittka for joint work on bumblebee flights as well as Peter Dieterich, Albrecht Schwab and Aleksei Chechkin for joint work on cell migration. He also thanks Nicholas Watkins for many inspiring discussions on Langevin dynamics, Sergei Fedotov for making him aware of Ross' letter to Person and Frederike Hanke for interesting hints on biological literature. Special thanks go to Luca Giuggioli for inviting him to the INI Programme, and INI for the hospitality, supported by EPSRC grant EP/R014604/1. Giving three talks during his visits to INI triggered the thoughts that led to this book chapter. A.G. and G.V. acknowledge sponsorship for this work by the US Office of Naval Research Global (award no. N62909-18-1-2170).

References

1. Dieterich, P., Lindemann, O., Moskopp, M.L., Tauzin, S., Huttenlocher, A., Klages, R., Chechkin, A., Schwab, A.: Anomalous diffusion and asymmetric tempering memory in neutrophil chemotaxis. PLOS Comput. Biol. **18**, 1–26 (2022)
2. Lenz, F., Ings, T.C., Chittka, L., Chechkin, A.V., Klages, R.: Spatiotemporal dynamics of bumblebees foraging under predation risk. Phys. Rev. Lett. **108**, 098103/1–5 (2012)
3. Parthasarathy, A.S.P.: Statistical analysis of sea turtle foraging. Master's Thesis, Queen Mary University of London, 2021
4. Bechinger, C., Di Leonardo, R., Löwen, H., Reichhardt, C., Volpe, G. and Volpe, G.: Active particles in complex and crowded environments. Rev. Mod. Phys. **88**, 045006 (2016)
5. Wehner, R.: Desert Navigator: The Journey of an Ant. Harvard University Press, Cambridge (2020)

6. Kays, R., Crofoot, M.C., Jetz, W., Wikelski, M.: Terrestrial animal tracking as an eye on life and planet. Science **348**, aaa2478 (2015)
7. Nathan, R., et al.: Big-data approaches lead to an increased understanding of the ecology of animal movement. Science **375**, eabg1780 (2022)
8. Brockmann, D., Hufnagel, L., Geisel, T.: The scaling laws of human travel. Nature **439**, 462–465 (2006)
9. Kumar, V., Torres, P.A.R., Eizaguirre, C., Palyulin, V.V., Klages, R.: in preparation (2024)
10. Cranna, V.: Karl Pearson and Sir Ronald Ross, 2015. Library, Archive and Open Research Services blog
11. Pearson, K.: Mathematical contributions to the theory of evolution—a mathematical theory of random migration. Biometric Ser. **3**, 54 (1906)
12. Brückner, D.B. and Broedersz, C.P.: Learning dynamical models of single and collective cell migration: a review. Rep. Progr. Phys. **87**, 056601 (2024)
13. Klages, R Cell migration: Beyond Brownian motion. Biophys. J. **123**, 1167–1169 (2024)
14. Schweitzer, F.: Brownian Agents and Active Particles. Springer, Berlin (2003)
15. Romanczuk, P., Bär, M., Ebeling, W., Lindner, B., Schimansky-Geier, L.: Active Brownian particles. Eur. Phys. J. Spec. Top. **202**, 1–162 (2012)
16. Ramaswamy, S.: The mechanics and statistics of active matter. Annu. Rev. Condes. Matter Phys. **1**, 323–345 (2010)
17. Marchetti, M.C., Joanny, J.F., Ramaswamy, S., Liverpool, T.B., Prost, J., Rao, M., Simha, R.A.: Hydrodynamics of soft active matter. Rev. Mod. Phys. **85**, 1143–1189 (2013)
18. Bernheim-Groswasser, A., Gov, N.S., Safran, S.A., Tzlil, S.: Living matter: mesoscopic active materials. Adv. Mater. **30**, 1707028 (2018)
19. Viswanathan, G.M., da Luz, M.G.E., Raposo, E.P., Stanley, H.E.: The Physics of Foraging. Cambridge University Press, Cambridge (2011)
20. Zaburdaev, V., Denisov, S., Klafter, J.: Lévy walks. Rev. Mod. Phys. **87**, 483–529 (2015)
21. Klages, R.: Search for food of birds, fish and insects. book chapter. In: Bunde, A., Caro, J., Kaerger, J., Vogl, G. (eds.) Diffusive Spreading in Nature, Technology and Society, 2nd edn., pp. 53–74. Springer, Berlin (2023)
22. Metzler, R., Klafter, J.: The random walk's guide to anomalous diffusion: a fractional dynamics approach. Phys. Rep. **339**, 1–77 (2000)
23. Metzler, R., Jeon, J.-H., Cherstvy, A.G. and Barkai, E.: Anomalous diffusion models and their properties: non-stationarity, non-ergodicity, and ageing at the centenary of single particle tracking. Phys. Chem. Chem. Phys. **16**, 24128–24164 (2014)
24. Klages, R., Radons, G., Sokolov, I.M. (eds.): Anomalous transport: Foundations and Applications. Wiley-VCH, Berlin (2008)
25. Nathan, R., Getz, W.M., Revilla, E., Holyoak, M., Kadmon, R., Saltz, D. and Smouse, P.E.: A movement ecology paradigm for unifying organismal movement research. Proc. Natl. Acad. Sci. **105**, 19052 (2008)
26. Méndez, V., Campos, D., Bartumeus, F.: Stochastic Foundations in Movement Ecology. Springer, Berlin (2014)
27. Joo, R., Picardi, S., Boone, M.E., Clay, T.A., Patrick, S.C., Romero-Romero, V.S., Basille, M.: Recent trends in movement ecology of animals and human mobility. Mov. Ecol. **10**, 26 (2022)
28. Patterson, T.A., Parton, A., Langrock, R., Blackwell, P.G., Thomas, L., King, R.: Statistical modelling of individual animal movement: an overview of key methods and a discussion of practical challenges. AStA Adv. Stat. Anal. **101**, 399–438 (2017)
29. Auger-Méthé, M., Newman, K., Cole, D., Empacher, F., Gryba, R., King, A.A., Leos-Barajas, V., Mills Flemming, J., Nielsen, A., Petris, G., Thomas, L.: A guide to state–space modeling of ecological time series. Ecol. Monogr. **91**, e01470 (2021)
30. Glennie, R., Adam, T., Leos-Barajas, V., Michelot, T., Photopoulou, T., McClintock, B.T.: Hidden Markov models: Pitfalls and opportunities in ecology. Methods Ecol. Evol. **14**, 43–56 (2023)
31. Codling, E.A., Plank, M.J., Benhamou, S.: Random walk models in biology. J. R. Soc. Interface **5**, 813–834 (2008)

32. Kareiva, P.M., Shigesada, N.: Analyzing insect movement as a correlated random walk. Oecologia **56**, 234–238 (1983)
33. Lenz, F., Chechkin, A.V., Klages, R.: Constructing a stochastic model of bumblebee flights from experimental data. PLoS ONE **8**, e59036/1–7 (2013)
34. te Vrugt, M, Wittkowski, R.: A review of active matter reviews (2024). preprint arXiv:2405.15751
35. Schweitzer, F.: An agent-based framework of active matter with applications in biological and social systems. Eur. J. Phys. **40**, 014003 (2019)
36. Langevin, P.: Sur la théorie du mouvement brownien. C.R. Acad. Sci. (Paris) **146**, 530–533 (1908). see also the English translation in Am. J. Phys. **65**, 1079 (1997)
37. Coffey, W., Kalmykov, Y.P., Waldron, J.T.: The Langevin Equation. World Scientific, Singapore (2004)
38. Ebeling, W., Schweitzer, F., Tilch, B.: Active Brownian particles with energy depots modeling animal mobility. BioSystems **49**, 17–29 (1999)
39. Howse, J.R., Jones, R.A., Ryan, A.J., Gough, T., Vafabakhsh, R., Golestanian, R.: Self-motile colloidal particles: From directed propulsion to random walk. Phys. Rev. Lett. **99**, 048102 (2007)
40. Koumakis, N., Maggi, C., Di Leonardo, R.: Directed transport of active particles over asymmetric energy barriers. Soft Matter **10**, 5695–5701 (2014)
41. Szamel, G.: Self-propelled particle in an external potential: existence of an effective temperature. Phys. Rev. E **90**, 012111 (2014)
42. Martin, D., O'Byrne, J., Cates, M.E., Fodor, É., Nardini, C., Tailleur, J., Van Wijland, F.: Statistical mechanics of active Ornstein-Uhlenbeck particles. Phys. Rev. E **103**, 032607 (2021)
43. Berg, H.C.: E. Coli in Motion. Springer, New York (2008)
44. Schnitzer, M.J.: Theory of continuum random walks and application to chemotaxis. Phys. Rev. E **48**, 2553–2568 (1993)
45. Khatami, M., Wolff, K., Pohl, O., Ejtehadi, M.R., Stark, H.: Active Brownian particles and run-and-tumble particles separate inside a maze. Sci. Rep. **6**, 1–10 (2016)
46. Lemaitre, E., Sokolov, I.M., Metzler, R., Chechkin, A.V.: Non-Gaussian displacement distributions in models of heterogeneous active particle dynamics. New J. Phys. **25**, 013010 (2023)
47. Kurzthaler, C., Leitmann, S., Franosch, T.: Intermediate scattering function of an anisotropic active Brownian particle. Sci. Rep. **6**, 36702 (2016)
48. Valani, R.N., Paganin, D.M.: Attractor-driven matter. Chaos **33**, 023125 (2023)
49. Pikovsky, A.: Deterministic active particles in the overactive limit. Chaos **33**, 113114 (2023)
50. Basu, U., Majumdar, S.N., Rosso, A., Schehr, G.: Active Brownian motion in two dimensions. Phys. Rev. E **98**, 062121 (2018)
51. Pearson, K.: The problem of the random walk. Nature **72**, 294, 342 (1905)
52. Viswanathan, G.M., Afanasyev, V., Buldyrev, S.V., Murphy, E.J., Prince, P.A., Stanley, H.E.: Lévy flight search patterns of wandering albatrosses. Nature **381**, 413–415 (1996)
53. Zaburdaev, V., Fouxon, I., Denisov, S., Barkai, E.: Superdiffusive dispersals impart the geometry of underlying random walks. Phys. Rev. Lett. **117**, 270601 (2016)
54. Viswanathan, G.M., Buldyrev, S.V., Havlin, S., da Luz, M.G., Raposo, E.P., Stanley, H.E.: Optimizing the success of random searches. Nature **401**, 911–914 (1999)
55. Edwards, A.M., Phillips, R.A., Watkins, N.W., Freeman, M.P., Murphy, E.J., Afanasyev, V., Buldyrev, S.V., da Luz, M.G., Raposo, E.P., Stanley, H.E., Viswanathan, G.M.:
Revisiting Lévy flight search patterns of wandering albatrosses, bumblebees and deer. Nature **449**, 1044–1048 (2007)
56. Pyke, G.H.: Understanding movements of organisms: it's time to abandon the Lévy foraging hypothesis. Meth. Ecol. Evol. **6**, 1 (2015)
57. Reynolds, A.M.: Current status and future directions of Lévy walk research. Biol. Open **7**, 03016 (2018)
58. Levernier, N., Textor, J., Bénichou, O. and Voituriez, R.: Inverse square Lévy walks are not optimal search strategies for $d \geq 2$. Phys. Rev. Lett. **124**, 080601 (2020)
59. Benhamou, S.: How many animals really do the lévy walk? Ecology **88**, 1962–1969 (2007)

60. Bénichou, O., Loverdo, C., Moreau, M., Voituriez, R.: Intermittent search strategies. Rev. Mod. Phys. **83**, 81–129 (2011)
61. Vilk, O., Orchan, Y., Charter, M., Ganot, N., Toledo, S., Nathan, R., Assaf, M.: Ergodicity breaking in area-restricted search of avian predators. Phys. Rev. X **12**, 031005 (2022)
62. Khadem, S.M.J., Klapp, S.H., Klages, R.: Search efficiency of discrete fractional Brownian motion in a random distribution of targets. Phys. Rev. Res. **3**, 023169 (2021)
63. Gomez-Solano, J.R., Sevilla, F.J.: Active particles with fractional rotational brownian motion. J. Stat. Mech.: Theor. Exp. **2020**, 063213 (2020)
64. Ings, T.C., Chittka, L.: Speed-accuracy tradeoffs and false alarms in bee responses to cryptic predators. Curr. Biol. **18**, 1520–1524 (2008)
65. Dieterich, P., Klages, R., Preuss, R., Schwab, A.: Anomalous dynamics of cell migration. PNAS **105**, 459–463 (2008)
66. Klimek, A., Mondal, D., Block, S., Sharma, P., Netz, R.R.: Data-driven classification of individual cells by their non-Markovian motion. Biophys. J. **123**, 1173–1183 (2024)
67. Roman Torres, P.A.: Environmental variation shapes life history traits of sea turtles: an ecological modelling approach. Ph.D. Thesis, Queen Mary University of London, 2022
68. Gentili, A., Klages, R., Volpe, G.: Anomalous diffusion of superparamagnetic walkers with tailored statistics (2025). preprint arXiv:2412.13960
69. Lucero-Azuara, N., Klages, R.: in preparation (2024)
70. Gardiner, C.: Stochastic Methods: A Handbook for the Natural and Social Sciences. Springer Series in Synergetics. Springer, Berlin (2009)
71. Watkins, N.W., Calel, R., Chapman, S.C., Chechkin, A., Klages, R., Stainforth, D.A.: The challenge of non-Markovian energy balance models in climate. Chaos **34**, 072105 (2024)
72. von Uexküll, J.: Umwelt und Innenwelt der Tiere. Springer, Berlin (1909)
73. Klatzky, R.L.: Allocentric and egocentric spatial representations: definitions, distinctions, and interconnections. book chapter. In: Freksa, C., Habel, C., Wender, K.F. (eds.) Spatial Cognition: An Interdisciplinary Approach to Representing and Processing Spatial Knowledge, pp. 1–17. Springer, Berlin (1998)
74. Edvardsen, V., Bicanski, A., Burgess, N.: Navigating with grid and place cells in cluttered environments. Hippocampus **30**, 220–232 (2020)
75. Abe, M.S.: Functional advantages of lèvy walks emerging near a critical point. PNAS **117**(39), 24336–24344 (2020)
76. Cheng, K.: Oscillators and servomechanisms in orientation and navigation, and sometimes in cognition. Proc. R. Soc. Lond. Ser. B, Biol. Sci. **289**(1974), 20220237 (2022)